Surface Impedance Boundary Conditions of High Order of Approximation for the Finite Integration Technique

Luca Di Rienzo[1], Nathan Ida[2], and Sergey Yuferev[3]

(1) Dipartimento di Elettrotecnica, Politecnico di Milano, P.zza L. da Vinci, 32, 20133, Milano, Italy; luca.dirienzo@etec.polimi.it
(2) Department of Electrical Engineering, The University of Akron, Akron, OH 44325-3904, USA; ida@uakron.edu
(3) Nokia Corp., P.O. Box 1000, Tampere FIN-34101, Finland; sergey.yuferev@nokia.com

Abstract — Time domain Surface Impedance Boundary Conditions (SIBCs) of high order of approximation relating the electric field integral along the edge of the computational cell and the magnetic flux through its facet are derived and implemented into the Finite Integration Technique (FIT). It enables such effects as curvature of the conductor surface and variation of the electromagnetic field along the interface to be accurately described in the formulation. As a result, accuracy of numerical results is improved and the application area is expanded as compared with formulations employing classical low order Leontovich SIBCs. Numerical results obtained using low- and high-order FIT-SIBC formulations are compared with analytical results to demonstrate the advantages of the proposed approach.

Keywords — Surface Impedance Boundary Conditions, Finite Integration Technique, Time Domain Methods, Approximate Boundary Conditions.

I. INTRODUCTION

Although the surface impedance concept has the reputation of a sophisticated numerical technique, it is actually based on well-known assumption, namely: the electromagnetic field distribution in the conductor's skin layer can be described as a damped plane wave propagating in the bulk of the conductor normal to its surface. In other words, the behavior of the electromagnetic field in the conducting region may be assumed to be known *a priori*. The electromagnetic field is continuous across the real conductor's surface, so the intrinsic impedance of the wave remains the same at the interface. Therefore, the ratio E_x/H_y (*Surface Impedance*) at the *xy*-plane of a dielectric/conductor interface is assumed to be equal to the intrinsic impedance of the plane wave propagating in the conductor, in the positive *z*-direction

$$\left.\frac{E_x}{H_y}\right|_{\text{interface}} = \left.\sqrt{\frac{j\omega_{source}\mu}{\sigma + j\omega_{source}\varepsilon}}\right|_{\sigma>>\omega\varepsilon} \approx \frac{1+j}{2}\omega_{source}\mu\delta\,,$$
$$\delta = \sqrt{\frac{2}{\omega_{source}\sigma\mu}}\,. \qquad (1)$$

The *surface* relation in (1), taking into account parameters of the conductor's material and the source, contains all necessary information about the field distribution in the conductor's *volume*. Thus it may be used as a boundary condition to the governing equations for the dielectric space that excludes the conductor from the region of solution and reduces the computational space to be discretized. It can be represented in another form relating normal and tangential magnetic fields at the interface.

The relation in (1) is usually referred to as Leontovich's SIBC. Although it has been widely used in combination with most numerical methods, it does not take into account curvature of the interface and variation of the field along the surface. SIBCs of high order of approximation allowing for both mentioned effects have been developed in frequency domain [1-2] and time domain [3] to improve accuracy and expand the application area of the surface impedance concept.

In the present paper time domain SIBCs of high order of approximation are derived in the state variables of the Finite Integration Technique (FIT) [4]. It extends results obtained in [5] where a low order SIBC has been implemented into the FIT.

II. THE FINITE INTEGRATION TECHNIQUE

The FIT, first proposed in [4], is based on the discretization of Maxwell equations in their integral form on two different staggered grids, a primary and a dual grid [6-7]. An example of the orthogonal dual mesh used in FIT is shown in Fig. 1.

Let L_i, S_i, V_i be the edges, facets, and volumes of the primary grid G and $\widetilde{L}_i$, $\widetilde{S}_i$, $\widetilde{V}_i$ the edges, facets, and volumes of the dual grid $\widetilde{G}$. Then, the state variables in FIT are defined as

$$\hat{e}_i = \int_{L_i} \vec{E} \cdot d\vec{l} \quad , \quad \hat{\tilde{b}}_i = \int_{S_i} \vec{B} \cdot d\vec{A} \ , \tag{2}$$

$$\hat{h}_i = \int_{\widetilde{L}_i} \vec{H} \cdot d\vec{l} \ , \quad \hat{\tilde{d}}_i = \int_{\widetilde{S}_i} \vec{D} \cdot d\vec{A} \ , \tag{3}$$

while the current flux and the electric charge are defined as

$$\hat{\tilde{j}}_i = \int_{\widetilde{S}_i} \vec{J} \cdot d\vec{A} \quad , \quad q_i = \int_{\widetilde{V}_i} q \cdot dV \ . \tag{4}$$

The discretized Maxwell equations are written in compact form in matrix notation as

$$\mathbf{C}\hat{\mathbf{e}} = -\frac{d}{dt}\hat{\tilde{\mathbf{b}}} \quad , \quad \widetilde{\mathbf{C}}\hat{\mathbf{h}} = \frac{d}{dt}\hat{\tilde{\mathbf{d}}} + \hat{\tilde{\mathbf{j}}} , \tag{5}$$

$$\mathbf{S}\hat{\tilde{\mathbf{b}}} = 0 \quad , \quad \widetilde{\mathbf{S}}\hat{\tilde{\mathbf{d}}} = \mathbf{q} , \tag{6}$$

where $\mathbf{C}$ and $\widetilde{\mathbf{C}}$ are the discrete equivalent of the continuous curl operator and $\mathbf{S}$ and $\widetilde{\mathbf{S}}$ are the discrete equivalent of the continuous divergence operator.

Equations (5) and (6) constitute the so-called *Maxwell's Grid Equations*.

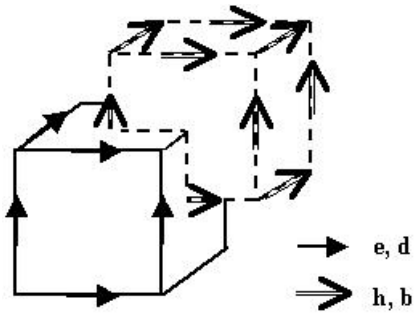

Fig. 1. One cell of the primary grid and one cell of the dual grid.

To complete the discrete system (5-6), the following three additional matrix operators (*material matrices*) must be introduced

$$\hat{\tilde{\mathbf{d}}} = \mathbf{M}_{\varepsilon}\hat{\mathbf{e}} \quad , \quad \hat{\tilde{\mathbf{j}}} = \mathbf{M}_{k}\hat{\mathbf{e}} \ , \ \hat{\mathbf{h}} = \mathbf{M}_{\mu^{-1}}\hat{\tilde{\mathbf{b}}} . \tag{7}$$

In a dual-orthogonal grid system, the primary edges and dual facets (as well as the dual edges and primary facets) intersect at 90°. In this case the material matrices are diagonal with entries

$$\mathbf{M}_{\varepsilon}(i,i) = \frac{\varepsilon_{eff,i}\widetilde{S}_i}{L_i} \quad , \quad \mathbf{M}_{k}(i,i) = \frac{\sigma_{eff,i}\widetilde{S}_i}{L_i} ,$$

$$\mathbf{M}_{\mu^{-1}}(i,i) = \frac{\widetilde{L}_i}{\mu_{eff,i}S_i} , \tag{8}$$

where $\varepsilon_{eff,i}$, $\sigma_{eff,i}$, and $\mu_{eff,i}$ are the material coefficients. These material relations are obtained introducing virtual field component $\vec{E}^{virt}$ at the intersection point of the dual facet and the primary edge and $\vec{B}^{virt}$ at the intersection point of primary facet and dual edge, so that

$$\hat{e}_i \cong E_i^{virt} \cdot L_i \quad , \quad \hat{\tilde{d}}_i \cong \varepsilon_{eff,i} E_i^{virt} \cdot \widetilde{S}_i ,$$

$$\hat{\tilde{b}}_i \cong B_i^{virt} \cdot S_i \quad , \quad \hat{h}_i = \mu_{eff,i}^{-1} B^{virt} \cdot \widetilde{L}_i . \tag{9}$$

Using a leap frog scheme, (5) are discretized in time as

$$\hat{\mathbf{e}}^{n+1/2} = \hat{\mathbf{e}}^{n-1/2} + \Delta t\left[\mathbf{M}_{\varepsilon}^{-1}\mathbf{C}^{T}\mathbf{M}_{\mu^{-1}}\hat{\tilde{\mathbf{b}}}^{n}\right],$$

$$\hat{\tilde{\mathbf{b}}}^{n+1} = \hat{\tilde{\mathbf{b}}}^{n} - \Delta t\mathbf{C}\hat{\mathbf{e}}^{n+1/2} . \tag{10}$$

III. SIBC OF HIGH ORDER OF APPROXIMATION IN TERMS OF FIT VARIABLES

In order to derive the SIBC of high order of approximation in the context of FIT, let us recall here that the approximate relation between the normal and tangential components of the magnetic flux density in the time domain can be written in the form [3]

$$B_{\eta}^{s} = \sum_{i=1}^{2} \frac{\partial}{\partial \xi_i} \left\{ T_1 \times B_{\xi_i}^{s} + \frac{d_{3-i} - d_i}{2 d_i d_{3-i}} T_2 \times B_{\xi_i}^{s} \right.$$
$$+ \frac{3d_{3-i}^2 - d_i^2 - 2d_i\, d_{3-i}}{8 d_i^2 d_{3-i}^2} T_3 \times B_{\xi_i}^{s}$$
$$\left. + \frac{1}{2} T_3 \times \left(- \frac{\partial^2 B_{\xi_i}^{s}}{\partial \xi_{3-i}^2} + \frac{\partial^2 B_{\xi_i}^{s}}{\partial \xi_i^2} + 2 \frac{\partial^2 B_{\xi_{3-i}}^{s}}{\partial \xi_i \partial \xi_{3-i}} \right) \right\}, \tag{11}$$

where the superscript "s" denotes quantities at the conductor surface, "*" denotes a time convolution product, d_k, $k=1,2$, are the local radii of curvature, and (ξ_1,ξ_2,η) are the principal curvature coordinates (Fig. 2).

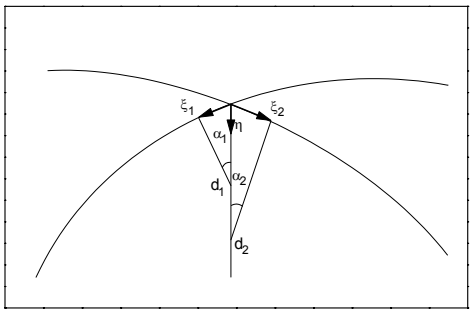

Fig. 2. Local orthogonal curvilinear coordinate systems related to the surface.

The time functions T_m, $m=1,2,3$ are defined as

$$T_1(t)=\sqrt{\frac{\mu_0}{\varepsilon_r\varepsilon_0}}I_0\left(\frac{\sigma t}{2\varepsilon_r\varepsilon_0}\right)\exp\left(-\frac{\sigma t}{2\varepsilon_r\varepsilon_0}\right),$$

$$T_2(t)=\frac{1}{\sigma}\left[1-\exp\left(-\frac{\sigma t}{\varepsilon_r\varepsilon_0}\right)\right],$$

$$T_3(t)=\frac{2t}{\sigma\sqrt{\varepsilon_r\varepsilon_0\mu_0}}I_1\left(\frac{\sigma t}{2\varepsilon_r\varepsilon_0}\right)\exp\left(-\frac{\sigma t}{2\varepsilon_r\varepsilon_0}\right).$$

The first term in (11) gives the SIBC of Leontovich's order of approximation in which the body's surface is considered as a plane and the field is assumed to be penetrating into the conductor only in the direction normal to the body's surface. The second and third terms give corrections taking into account the curvature of the conductor surface. The last term allows for the electromagnetic field diffusion in directions tangential to the conductor's surface.

Let us analyze the expression in the last term of the right hand side of (11)

$$\sum_{i=1}^{2}\frac{\partial}{\partial\xi_i}\left(-\frac{\partial^2 B^s_{\xi_i}}{\partial\xi_{3-i}^2}+\frac{\partial^2 B^s_{\xi_i}}{\partial\xi_i^2}+2\frac{\partial^2 B^s_{\xi_{3-i}}}{\partial\xi_i\partial\xi_{3-i}}\right)=$$

$$=\frac{\partial}{\partial\xi_1}\left(\frac{\partial^2 B^s_{\xi_1}}{\partial\xi_1^2}+\frac{\partial^2 B^s_{\xi_1}}{\partial\xi_2^2}\right)+\frac{\partial}{\partial\xi_2}\left(\frac{\partial^2 B^s_{\xi_2}}{\partial\xi_1^2}+\frac{\partial^2 B^s_{\xi_2}}{\partial\xi_2^2}\right)=$$

$$=\frac{\partial}{\partial\xi_1}\nabla^2 B^s_{\xi_1}+\frac{\partial}{\partial\xi_2}\nabla^2 B^s_{\xi_2}=\nabla\cdot\left[\left(\vec{n}\times\nabla^2\vec{B}^s\right)\times\vec{n}\right]=$$

$$=\vec{n}\cdot\nabla\times\left(\vec{n}\times\nabla^2\vec{B}^s\right), \qquad (12)$$

where the unit normal vector $\vec{n}$ is directed out of the body. Here the Laplacian operator of a vector field $\vec{f}(\xi_1,\xi_2)$ is defined as follows

$$\nabla^2\vec{f}=\sum_{i=1}^{3}\vec{a}_{\xi_i}\nabla^2 f_{\xi_i}\ .$$

The use of (12) allows (11) to be represented in the form:

$$\begin{aligned}B^s_\eta=&\sum_{i=1}^{2}\frac{\partial B^s_{\xi_i}}{\partial\xi_i}\times T_1+\sum_{i=1}^{2}v_i\frac{\partial B^s_{\xi_i}}{\partial\xi_i}\times T_2\\&+\sum_{i=1}^{2}w_i\frac{\partial B^s_{\xi_i}}{\partial\xi_i}\times T_3+\frac{1}{2}\sum_{i=1}^{2}\frac{\partial\nabla^2 B^s_{\xi_i}}{\partial\xi_i}\times T_3,\end{aligned} \qquad (13)$$

where

$$v_i=\frac{d_{3-i}-d_i}{2d_i d_{3-i}}\ ,\ w_i=\frac{3d_{3-i}^2-d_i^2-2d_i\,d_{3-i}}{8d_i^2 d_{3-i}^2},\ i=1,2. \qquad (14)$$

Performing integration on both sides of (13) over the facet ABCD of the cell shown in Fig. 3, one obtains:

$$\hat{\hat{b}}_0=\iint_{S_{b0}}B^s_\eta ds=\iint_{S_{b0}}\left(\sum_{i=1}^{2}\frac{\partial B^s_{\xi_i}}{\partial\xi_i}\times T_1+\sum_{i=1}^{2}v_i\frac{\partial B^s_{\xi_i}}{\partial\xi_i}\times T_2+\right.$$

$$\left.+\sum_{i=1}^{2}w_i\frac{\partial B^s_{\xi_i}}{\partial\xi_i}\times T_3+\frac{1}{2}\sum_{i=1}^{2}\frac{\partial\nabla^2 B^s_{\xi_i}}{\partial\xi_i}\times T\right)ds\,. \qquad (15)$$

Suppose the coordinates of points D and B in the $\xi_1\xi_2$-plane are (ξ_{10},ξ_{20}) and $(\xi_{10}+\Delta\xi_1,\xi_{20}+\Delta\xi_2)$, respectively (here $\Delta\xi_1=AB=CD$ and $\Delta\xi_2=DA=BC$). Surface integrals appearing in (15) can be discretized as follows

$$\iint_{S_{b0}} \sum_{i=1}^{2} v_i \frac{\partial B^s_{\xi_i}}{\partial \xi_i} ds = \Delta\xi_1 \Delta\xi_2 \sum_{i=1}^{2} v_i \frac{\partial B^s_{\xi_i}}{\partial \xi_i} =$$

$$= v_1 \left[B^s_{\xi_1}(\xi_{10} + \Delta\xi_1) - B^s_{\xi_1}(\xi_{10}) \right] \Delta\xi_2 +$$

$$+ v_2 \left[B^s_{\xi_2}(\xi_{20} + \Delta\xi_2) - B^s_{\xi_2}(\xi_{20}) \right] \Delta\xi_1 =$$

$$= v_1 B_1^{virt} L_{DA} + v_1 B_3^{virt} L_{BC} + v_2 B_2^{virt} L_{AB} + v_2 B_4^{virt} L_{CD} =$$

$$= v_1 \hat{\hat{b}}_1 \frac{L_{e_1}}{S_{b_1}} + v_1 \hat{\hat{b}}_3 \frac{L_{e_3}}{S_{b_3}} + v_2 \hat{\hat{b}}_2 \frac{L_{e_2}}{S_{b_2}} + v_2 \hat{\hat{b}}_4 \frac{L_{e_4}}{S_{b_4}}, \qquad (16)$$

where

$L_{e1} = DA$, $L_{e2} = AB$, $L_{e3} = BC$, $L_{e4} = CD$,

$S_{b1} = S_{ADD'A'}$, $S_{b2} = S_{ABB'A'}$, $S_{b3} = S_{BCC'B'}$,

$S_{b4} = S_{CDD'C'}$.

Performing the integration of the other terms in (15) in the same way, one obtains:

$$\hat{\hat{b}}_0 = \iint_{S_{b0}} B^s_\eta ds$$

$$= \sum_{k=1}^{4} \frac{L_{e_k}}{S_{b_k}} \left(\hat{\hat{b}}_k \times T_1 + v_k \hat{\hat{b}}_k \times T_2 + w_k \hat{\hat{b}}_k \times T_3 + \frac{1}{2} \nabla^2 \hat{\hat{b}}_k \times T_3 \right) \qquad (17)$$

where $v_1 = v_3$, $v_2 = v_4$, $w_1 = w_3$, and $w_2 = w_4$.

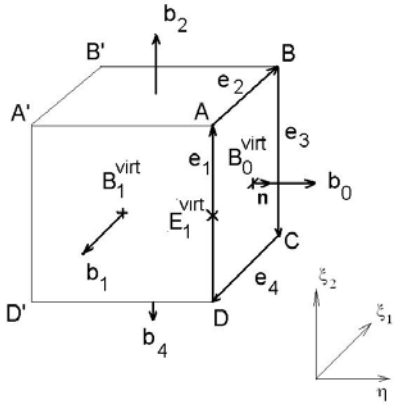

Fig. 3. Cartesian computational cell used in the FIT.

Substituting (17) into Faraday's law, we obtain the relation between $\hat{e}_k = \int_{L_{e_k}} \vec{E} \cdot d\vec{l}$ and $\hat{\hat{b}}_k = \iint_{S_{b_k}} \vec{B} \cdot \vec{n} ds$, $k=1,2,\ldots 4$

$$\hat{e}_k = \frac{L_{e_k}}{S_{b_k}} \frac{\partial}{\partial t} \left(\hat{\hat{b}}_k \times T_1 + v_k \hat{\hat{b}}_k \times T_2 + w_k \hat{\hat{b}}_k \times T_3 + \frac{1}{2} \nabla^2 \hat{\hat{b}}_k \times T_3 \right) =$$

$$= \frac{L_{e_k}}{S_{b_k}} \left(\hat{\hat{b}}_k \times T_1' + v_k \hat{\hat{b}}_k \times T_2' + w_k \hat{\hat{b}}_k \times T_3' + \frac{1}{2} \nabla^2 \hat{\hat{b}}_k \times T_3' \right) \qquad (18)$$

where

$$T_1'(t) = \left(\frac{1}{\mu_0 \varepsilon_r \varepsilon_0} \right)^{1/2} \left\{ \delta(t) + \right.$$

$$\left. + \frac{\sigma}{2\varepsilon_r \varepsilon_0} \left[I_1\left(\frac{\sigma t}{2\varepsilon_r \varepsilon_0} \right) - I_0\left(\frac{\sigma t}{2\varepsilon_r \varepsilon_0} \right) \right] \exp\left(-\frac{\sigma t}{2\varepsilon_r \varepsilon_0} \right) \right\},$$

$$T_2'(t) = \frac{1}{\mu_0 \varepsilon_r \varepsilon_0} \exp\left(-\frac{\sigma t}{\varepsilon_r \varepsilon_0} \right),$$

$$T_3'(t) = \frac{t}{\mu_0 \varepsilon_r \varepsilon_0 \sqrt{\varepsilon_r \varepsilon_0 \mu_0}} \left[I_0\left(\frac{\sigma t}{2\varepsilon_r \varepsilon_0} \right) - I_1\left(\frac{\sigma t}{2\varepsilon_r \varepsilon_0} \right) \right]$$

$$\times \exp\left(-\frac{\sigma t}{2\varepsilon_r \varepsilon_0} \right).$$

The third derivatives cannot be approximated within one computational cell shown in Fig. 3, so quantities defined in the surrounding cells of the computational grid must be used. Let p and q be ordinal numbers of the current cell in ξ_1 and ξ_2 directions, respectively. In the case of cartesian grid $L_{e_1} = L_{e_3}$ and $L_{e_2} = L_{e_4}$ so $\nabla^2 \hat{\hat{b}}_i^{p,q}$ can be approximated as follows:

$$\nabla^2 \hat{\hat{b}}_1^{p,q} = \left(\hat{\hat{b}}_1^{p+1,q} - 2\hat{\hat{b}}_1^{p,q} + \hat{\hat{b}}_1^{p-1,q} \right) \Big/ \left(L_{e_1} \right)^2, \qquad (19a)$$

$$\nabla^2 \hat{\hat{b}}_2^{p,q} = \left(\hat{\hat{b}}_2^{p,q+1} - 2\hat{\hat{b}}_2^{p,q} + \hat{\hat{b}}_2^{p,q-1} \right) \Big/ \left(L_{e_2} \right)^2, \qquad (19b)$$

$$\nabla^2 \hat{\hat{b}}_3^{p,q} = \left(\hat{\hat{b}}_3^{p+1,q} - 2\hat{\hat{b}}_3^{p,q} + \hat{\hat{b}}_3^{p-1,q} \right) \Big/ \left(L_{e_1} \right)^2, \qquad (19c)$$

$$\nabla^2 \hat{\hat{b}}_4^{p,q} = \left(\hat{\hat{b}}_4^{p,q+1} - 2\hat{\hat{b}}_4^{p,q} + \hat{\hat{b}}_4^{p,q-1} \right) \Big/ \left(L_{e_2} \right)^2 . \quad (19d)$$

Substitution of (19a-d) into (18) finally yields the relations between $\hat{e}_k^{p,q}$ and $\hat{\hat{b}}_k^{p,q}$ for the current cell

$$\hat{e}_k^{p,q} = \left[\begin{array}{l} \hat{\hat{b}}_k^{p,q} \times T_1' + v_k \hat{\hat{b}}_k^{p,q} \times T_2' + w_k \hat{\hat{b}}_k^{p,q} \times T_3' \\ + \dfrac{L_{e_k}}{S_{b_k}} \dfrac{1}{2} \left(\hat{\hat{b}}_k^{p+1,q} - 2\hat{\hat{b}}_k^{p,q} + \hat{\hat{b}}_k^{p-1,q} \right) \Big/ \left(L_{e_k} \right)^2 \times T' \end{array} \right] . \quad (20)$$

The SIBC of low order of approximation derived in [5] is given only by the first term of the right hand side of (20)

$$\hat{e}_k^{p,q} = \frac{L_{e_k}}{S_{b_k}} \hat{\hat{b}}_k^{p,q} \times T' . \quad (21)$$

IV. NUMERICAL EXAMPLE AND VALIDATION

A canonical 2D example is considered, for which the analytical solution is known [8]: a line current *I(t)* placed at point $(0, y_s)$ radiating over a half-space (Fig. 4).

Although the high order SIBC accurately models the curvature of the surface, the test case has been chosen with planar surface in order not to introduce the typical error of FIT with cartesian grid known as the "staircase effect". As a matter of fact, the modeling of curved surfaces by means of high order SIBC and FIT would require a conformal scheme. In the proposed example the improvement in accuracy given by the SIBC of high order of approximation is only due to the modeling of the variation of the electromagnetic field along the surface, which is not accounted for by the low order SIBC of the Leontovich type. Hence, since the surface is planar, coefficients v_i and w_i in (18) are zero.

The computational domain (the dielectric half-space) is discretized into a 100 x 100 Cartesian grid made of one layer of 3D Yee cubic cells with side length Δ=0.015 m. Mur's first order absorbing boundary conditions are used at the other boundaries. Time convolutions in (18) are computed recoursively applying the Prony's method, as proposed in [9].

The following current pulse is considered

$$I(t) = \frac{t - \tau_0}{\tau} e^{-\left(\frac{t-\tau_0}{\tau} \right)^2} , \quad (22)$$

with $\tau = 40\Delta t$, $\tau_0 = 12\Delta t$, where the time step Δt was chosen as $\Delta t = \Delta x / 2c_0$. The electric field at point $(x_0, 0)$ is computed using the low order SIBC, the high order SIBC and the analytical solution (Fig. 5-6). As can be noted, at low values of conductivity (σ = 0.1 S/m) and when the filamentary source is near to the surface, the SIBC of low order does not give accurate results, while a better accuracy is reached by means of the present formulation. In the cases of higher values of conductivity (σ =1 S/m, σ =10 S/m), as shown in [4], the low order SIBC is accurate enough.

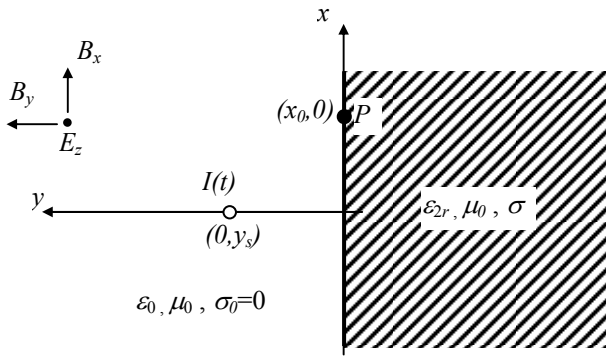

Fig. 4. Geometry of the test problem.

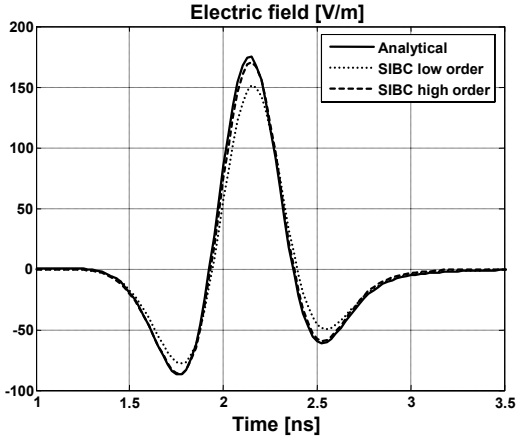

Fig. 5. Electric field at the observation point for y_s=10Δ; x_s=20Δ; σ= 0.1 S/m.

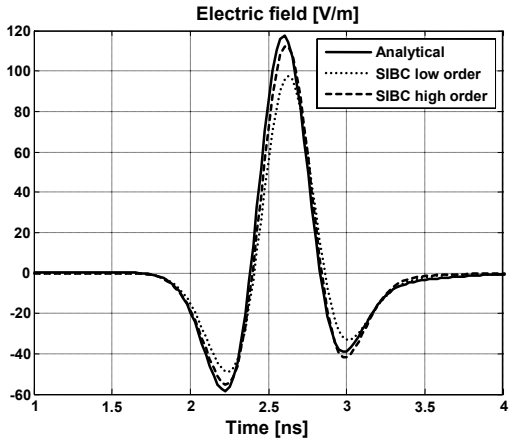

Fig. 6. Electric field at the observation point for y_s=10Δ; x_s=30Δ; σ= 0.1 S/m.

V. CONCLUSIONS

The 2D numerical example has shown the improvement in accuracy of the proposed formulation compared to the corresponding formulation published in [5] employing low order SIBC. Even if FIT with Cartesian grid is computationally equivalent to FDTD, in the paper high order SIBCs have been expressed directly in FIT state variables and in future work they can be generalized to non cartesian grids and implemented in conformal schemes.

REFERENCES

[1] S. M. Rytov, "Calculation of skin effect by perturbation method," *Zhurnal Experimental'noi I Teoreticheskoi Fiziki*, vol. 10, pp.180-189, 1940.

[2] K. M. Mitzner, "An integral equation approach to scattering from a body of finite conductivity," *Radio Science*, vol. 2, pp. 1459-1470, 1967.

[3] S. Yuferev and N. Ida, "Time domain surface impedance boundary conditions of high order of approximation," *IEEE Trans. on Magnetics*, vol. 34, no. 5, pp. 2605 – 2608, September 1998.

[4] T. Weiland, "A discretization method for the solution of Maxwell's equations for six-component fields," *Electronic and Communication (AEÜ)*, vol. 31, pp. 116-120, 1977.

[5] S. Yuferev, L. Di Rienzo, and N. Ida, "Surface impedance boundary conditions for the finite integration technique," *IEEE Trans. on Magnetics*, vol. 42, no. 4, pp. 823-826, April 2006.

[6] T. Weiland, "Advances in FIT/FDTD modeling," *Proceedings of 18th Annual review of progress in applied computational electromagnetics*, pp. 1.1-1.14, 2002.

[7] T. Weiland, "Time domain electromagnetic field computations with finite difference methods," *International Journal of Numerical Modelling: Electronic Networks, Devices and Fields*, vol. 9, pp. 295-319, 1996.

[8] G. S. Smith, "On the skin effect approximation," *Am. J. Phys.*, vol. 58, no. 10, pp. 996-1002, 1990.

[9] K. S. Oh and J. E. Schutt-Aine, "An efficient implementation of surface impedance boundary conditions for the finite-difference time-domain method," *IEEE Trans. Antennas Propagat.*, vol. 43, no. 7, pp. 660-666, 1995.

Luca Di Rienzo was born in Foggia, Italy, in 1971. He received the Laurea degree in 1996 and the Ph. D. degree in 2001, both in electrical engineering and from Politecnico di Milano, Milano, Italy.
He is currently assistant professor of electrical engineering with the Dipartimento di Elettrotecnica of Politecnico di Milano. At present, his research interests are in the field of computational electromagnetics and include magnetic inverse problems and surface impedance boundary conditions. He is also involved in electromagnetic compatibility problems using commercial software packages.

Nathan Ida is currently Professor of electrical engineering at The University of Akron, Akron, Ohio, USA, where he has been since 1985. His current research interests are in the areas of numerical modeling of electromagnetic fields, electromagnetic wave propagation, nondestructive testing of materials at low and microwave frequencies and in computer algorithms. Dr. Ida received his B.Sc. in 1977 and M.S.E.E. in 1979 from the Ben-Gurion University in Israel and his Ph.D. from Colorado State University in 1983.

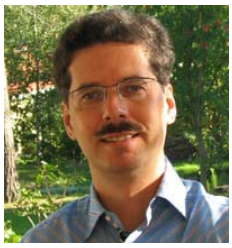

Sergey Yuferev was born in St. Petersburg, Russia, in 1964. He received MSc degree in computational fluid mechanics from St. Petersburg Technical University in 1987 and PhD degree in computational electromagnetics from A.F. Ioffe Institute in 1992. From 1987 to 1998 he was with Dense Plasma Dynamics Laboratory of A. F. Ioffe Institute. From 1999 to 2000 he was Visiting Associate Professor at The University of Akron, Ohio. Since 2000, he has been with Nokia Corp., Finland. His current research interests include numerical and analytical methods of computational electromagnetics and their application to EMC/EMI problems of mobile phones.